

1 Measurements of single and double D^0 meson 2 production in pp collisions at $\sqrt{s} = 13.6$ TeV

3 **Andrea Tavira García^{a,*} for the ALICE collaboration**

4 ^a*IJCLab, Université Paris-Saclay,*

5 *15 rue Georges Clemenceau, Orsay, France*

6 *E-mail: tavira-garcia@ijclab.in2p3.fr*

7 D-meson production measurements in pp collisions are used to test perturbative quantum chromodynamics (pQCD) calculations. This contribution reports the preliminary results of the non-prompt D^0 fraction at midrapidity in the transverse momentum range $p_T < 24$ GeV, measured in pp collisions at $\sqrt{s} = 13.6$ TeV, using data from the LHC Run 3. Results are compared to the predictions of EPOS and various modes of PYTHIA simulations. Additionally, the double production of D mesons allows to study single (SPS) and double parton scattering (DPS). Like-sign meson pairs are expected to be predominantly produced by DPS processes, while opposite-sign pairs are more likely to be created via SPS. The status of the measurement of double production of D^0 mesons in pp collisions at $\sqrt{s} = 13.6$ TeV is also reported.

ICHEP

17-24 July 2024

Prague, Czechia

*Speaker

8 1. Introduction

9 This contribution reports some of the first results of the ALICE Collaboration involving D mesons
 10 in pp collisions at $\sqrt{s} = 13.6$ TeV exploiting Run 3 data. In particular, the measurement of the non-
 11 prompt D⁰ fraction and the status of the double D⁰ production measurement are reported. D⁰ mesons
 12 and their charge conjugates are reconstructed via their hadronic decay channel, $D^0 \rightarrow K^- \pi^+$, using
 13 the central barrel, which covers the pseudorapidity range $|\eta| < 0.9$. The main detectors employed
 14 include the Inner Tracking System (ITS), used for tracking and vertexing; the Time Projection
 15 Chamber (TPC), used for tracking and particle identification (PID); and the Time-of-Flight (TOF)
 16 detector, used for particle identification. Collisions were triggered using the Fast-Interaction-Trigger
 17 (FIT). More details are provided in Ref.[1].

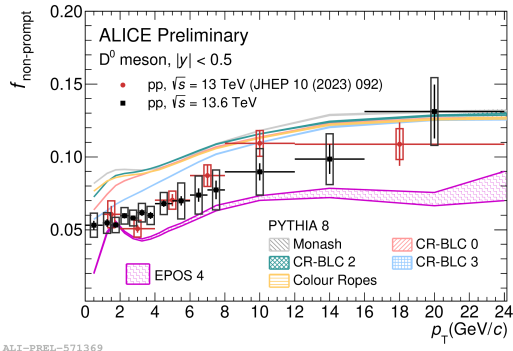
18 2. Non-prompt D⁰-meson fraction calculation

19 Measurements of the fraction of non-prompt D⁰ mesons allow us to test perturbative QCD (pQCD)
 20 calculations in the beauty sector. In ALICE, these measurements were already performed at
 21 midrapidity exploiting Run 2 data at $\sqrt{s} = 13$ TeV [1]. The measurement of the non-prompt D⁰
 22 fraction in pp collisions at $\sqrt{s} = 13.6$ TeV is reported here down to $p_T = 0$ and with finer granularity
 23 with respect to Run 2 data.

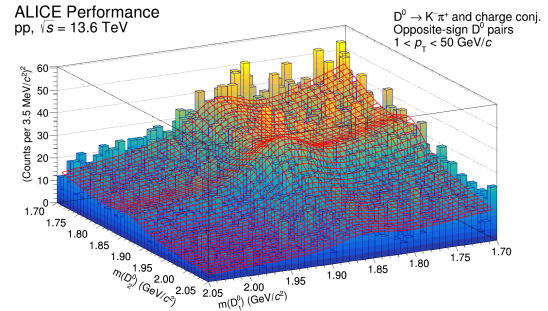
24 To extract the D⁰ signals, a set of boosted decision tree (BDT) algorithms was employed in different
 25 p_T intervals, making use of topological variables exploiting the D⁰ displaced decay topology and
 26 particle-identification information on the D⁰ daughter tracks. They were used to separate between
 27 prompt D⁰, non-prompt D⁰, and combinatorial background candidates in the measured p_T interval.
 28 The candidates for the first two classes used in the training were obtained from Monte Carlo
 29 (MC) simulations. In contrast, background candidates were obtained from the sidebands of the
 30 data invariant-mass distribution. Once the signals were extracted, a data-driven method known
 31 as cut-variation was used to determine the non-prompt fraction. This approach considers that the
 32 D⁰-meson yield is composed of a prompt and non-prompt component, whose corrected values can
 33 be computed as in Eq.1. In this equation, $(\text{Acc} \times \epsilon)$ is the acceptance of the detector multiplied by the
 34 efficiency, which can be obtained from MC simulations, $N_{(\text{non-})\text{prompt}}$ is the number of (non-)prompt
 35 candidates, and Y is the measured raw yield, extracted from the invariant-mass distribution of $K\pi$
 36 pairs. This method tests different BDT scores to vary the $(\text{Acc} \times \epsilon)$ and the relative contribution
 37 from the prompt and non-prompt components in Eq.1 and obtain a system of equations. An iterative
 38 procedure was performed in order to solve the system by minimising the χ^2 and extract the fraction.

$$(\text{Acc} \times \epsilon)_i^{\text{prompt}} \cdot N_{\text{prompt}} + (\text{Acc} \times \epsilon)_i^{\text{non-prompt}} \cdot N_{\text{non-prompt}} = Y_i \quad (1)$$

39 The result of the non-prompt D⁰ fraction at $\sqrt{s} = 13.6$ TeV can be seen in Fig. 1a. The Run 3 results,
 40 in black, are compared to the previous Run 2 measurement, reported in red, and are compatible with
 41 each other. Results are also compared with theoretical calculations using EPOS 4 [3] and PYTHIA
 42 8 [2] with different tunes. As it can be observed, the measurement lies between PYTHIA and EPOS
 43 predictions. Overall, the Run 3 results extend the p_T coverage and granularity, providing tighter
 44 constraints to distinguish different hadronisation implementations.



(a) Non-prompt fraction, $f_{\text{non-prompt}}$, as a function of p_T in the $p_T < 24$ GeV/c range.



(b) Invariant-mass distribution of opposite-sign D^0 pairs, with a fit function superimposed.

Figure 1: (a) Non-prompt fraction as a function of p_T ; (b) Invariant-mass distribution of opposite-sign D^0 pairs.

45 3. Double production of D^0 mesons

46 Double D^0 -meson production measurements provide information on charm production from double-
 47 parton scattering (DPS). To distinguish the contribution to double- D^0 production from single-parton
 48 scattering (SPS) and DPS, it is possible to compare the cross-sections from opposite-sign and like-
 49 sign pairs, where the latter are expected to be dominated by DPS. This contribution presents a
 50 performance plot of the 2-dimensional invariant mass fit for opposite-sign D^0 pairs, which can be
 51 seen in 1b.

52 4. Conclusions

53 In this contribution, we presented the current status of measurements for single and double D^0
 54 meson production using ALICE Run 3 data. First, the fraction of non-prompt D^0 mesons was
 55 estimated, yielding the preliminary results shown in Figure 1a, which are compared with earlier
 56 results and theoretical predictions. Afterwards, the analysis progress on double- D^0 production was
 57 discussed, setting the stage for upcoming results.

58 References

- 59 [1] ALICE Collaboration. *JHEP* 10 (2023), p. 092. DOI: [10.1007/JHEP10\(2023\)092](https://doi.org/10.1007/JHEP10(2023)092). arXiv:
 60 [2302.07783](https://arxiv.org/abs/2302.07783) [nucl-ex].
- 61 [2] Torbjörn Sjöstrand et al. *Computer Physics Communications* 191 (2015), pp. 159–177. DOI:
 62 [10.1016/j.cpc.2015.01.024](https://doi.org/10.1016/j.cpc.2015.01.024).
- 63 [3] K. Werner. *Phys. Rev. C* 108 (6 Dec. 2023), p. 064903. DOI: [10.1103/PhysRevC.108.](https://doi.org/10.1103/PhysRevC.108.064903)
 64 [064903](https://doi.org/10.1103/PhysRevC.108.064903).